



# Unusual variation of temperature factor of uranium dioxide at high temperature

Hiroyuki Serizawa<sup>a,\*</sup>, Kousaku Fukuda<sup>a</sup>, Tetuo Shiratori<sup>a</sup>, Takeo Fujino<sup>b</sup>, Nobuaki Sato<sup>b</sup>, Kohta Yamada<sup>b</sup>

<sup>a</sup>Japan Atomic Energy Research Institute, Tokai-mura, Naka-Gun, Ibaraki-ken 319-11, Japan

<sup>b</sup>Institute for Advanced Materials Processing, Tohoku University, Sendai 980, Japan

## Abstract

High temperature behavior of  $\text{UO}_2$  was examined by X-ray diffraction. The temperature factor of  $\text{UO}_2$  was evaluated at room temperature and at high temperatures from 1003 to 1573 K. Two types of factors were calculated: the overall temperature factor of U and O atoms, designated as  $B$ ; and the temperature factor of U atom,  $B_U$ . In both cases, the value of the factors increased with increasing temperature up to ca. 1400 K. However, an anomalous decrease in these factors was detected above 1400 K. X-ray Debye temperature,  $\theta$ , was derived from the temperature factors as a function of temperature. Corresponding to the anomaly of the temperature factor,  $\theta$  increased atypically at the temperature higher than ca. 1400 K. © 1998 Elsevier Science S.A.

**Keywords:**  $\text{UO}_2$ ; Temperature factor; X-ray diffraction; High temperature

## 1. Introduction

The thermodynamic properties of solid phase uranium dioxide,  $\text{UO}_2$ , have been of considerable interest for its practical use as a nuclear fuel. It has been shown that  $\text{UO}_2$  exhibits an anomalous increase in the specific heat capacity,  $C_p$ , above 1400 K, which should be accounted for by some additional excitation process [1–3]. Some previous works attributed the anomaly to the formation of Frenkel defects in cation sublattice similar to that developed for the halides with  $\text{CaF}_2$ -type crystal structure [4–6]. On the other hand, the creation of the electronic disorder, or the electron–hole (e–h) pairs, through the reaction of electron transfer,  $2\text{U}^{4+} \rightarrow \text{U}^{3+} + \text{U}^{5+}$ , has also been proposed as the principal cause of the anomaly [7–11]. Relative contribution of these two kinds of defect formations is still in question.

The temperature factor of  $\text{UO}_2$  at high temperature has been reported by several workers through neutron diffraction method [6,12,13]. Willis [13] measured the temperature factor of  $\text{UO}_2$  up to 1400 K and confirmed that the Debye temperature is almost constant below 1400 K. Hutchings et al. [6] and Albinati et al. [12] conducted the measurement at higher temperature. However, the data at

around 1400 to 1600 K in which we are interested are still lacking.

In the present work, we carried out high temperature X-ray diffraction measurement of  $\text{UO}_2$  at temperatures from 1003 to 1573 K. The two kinds of temperature factors, overall temperature factor and temperature factor of uranium atom, were evaluated; the temperature dependence of these factors were examined. X-ray Debye temperature of  $\text{UO}_2$  was also calculated using the latter factor.

## 2. Experimental

The experimental apparatus used in this work was a Rigaku model No. 2315c1 high temperature X-ray diffractometer attachment mounted on a theta-theta goniometer system (Geigerflex DXG3) with a RINT operation system. The sample was placed on a graphite sample holder, which also worked as a resistive heating element. The temperature was measured on the surface of the sample with a pyrometer. The XRD measurements were conducted with  $\text{Cu K}_\alpha$  radiation monochromatized using the (002) plane of curved graphite. The slit width was  $0.5^\circ$  for both divergence and scatter slits.

Stoichiometric  $\text{UO}_2$  was obtained by reduction of  $\text{U}_3\text{O}_8$  in  $\text{He}/4\%\text{H}_2$  atmosphere at  $900^\circ\text{C}$ . After the  $\text{UO}_2$  sample

\*Corresponding author. Tel.: +81 29 2648421; fax: +81 29 2648478; e-mail: serizawa@popsvr.tokai.go.jp

was set in the heating attachment, it was evacuated and filled with He/4% H<sub>2</sub> gas mixture. This cycle was repeated three or four times. The inlet gas was purified by passing through a dry ice trap to eliminate the moisture. The sample was heated in the stream of the gas mixture. The line profiles were taken at room temperature, 1003, 1133, 1323, 1473, 1523, 1533 and 1573 K. When the intended temperature was attained, the geometrical arrangement of the sample holder was adjusted so that an X-ray source, the sample and a detector are all onto the focusing circle. The sample and sample holder used in high temperature measurement were replaced by new ones for each run. The measurement at room temperature was, however, carried out followed by that at 1533 K using the same sample and sample holder.

The integrated intensity of each diffraction peak for the determination of overall temperature factor was calculated with XRD pattern measured by fixed time method for the period of 5 s at each angle of 0.01° width in the neighborhood of each reflection. The measurement was carried out for all of the reflections observed in the diffraction angle between 30° and 140° except for three peaks indexed as (511), (442) and (620). This is because the reflections from (511) and (422) planes overlap with those from (333) and (600), respectively, and the broad scattering from the sample holder was obstructive to the evaluation of the intensity from the (620) plane. The XRD data for Rietveld analysis was also corrected by the fixed time method at diffraction angles between 30° and 140°.

### 3. Theoretical treatment

#### 3.1. Evaluation of overall temperature factor

The overall temperature factor was obtained by a conventional method that was outlined by Buerger [14]. The method needs the measurement of the integrated intensities of many diffraction peaks at a fixed temperature.

The integrated intensity,  $I$ , of Bragg reflection from the sample can be given by

$$I = KL_p P |F|_{hkl}^2 \quad (1)$$

where  $K$  is a constant;  $L_p$  is the Lorentz-polarization factor which is a function of the Bragg angle;  $P$  is the multiplicity factor; and  $|F|$  is the modulus of the structure factor. For UO<sub>2</sub>, since uranium atom has a much larger mass than oxygen atom, the respective Debye–Waller factors should be significantly different. However, to the first approximation, let the Debye–Waller factor of each atom be the same. Then, Eq. (1) becomes a simple form:

$$I = KL_p P |\Sigma f_a|^2 e^{-2B(\sin^2\theta/\lambda^2)} \quad (2)$$

where  $f_a$ ,  $B$ ,  $\theta$ ,  $\lambda$  are the atomic scattering factor of each

component atom, the overall temperature factor, Bragg angle and wavelength of the X-ray, respectively. The experimental structure factor,  $F_{\text{corr}}$ , is obtained from Eq. (2) using measured integrated intensity,  $I$ , as shown below:

$$|F_{\text{corr}}|^2 = \frac{I}{L_p P} = K |\Sigma f_a|^2 e^{-2B(\sin^2\theta/\lambda^2)} \quad (3)$$

where  $B$  is the overall temperature factor. It follows that the slope of the plot of  $\ln(|F_{\text{corr}}|^2/|\Sigma f_a|^2)$  versus  $\sin^2\theta/\lambda^2$  yields the value of  $-2B$ .

#### 3.2. Evaluation of temperature factor of each component atom

The temperature factor of each component atom can be evaluated simultaneously by Rietveld analysis. In the present work, we used 'RIETAN96' code developed by Izumi [15]. However, since the atomic scattering factor of oxygen atom is too small compared with that of uranium atom, the refinement of the temperature factor of oxygen atom,  $B_O$ , was difficult. Thus, fixing the value of  $B_O$  to that reported by Hutchings et al. [6], we conducted the refinement only for the temperature factor of uranium atom,  $B_U$ . The discrepancy index of the final refinement,  $R_F$ , was less than 5%, which means that the refinement was done successfully.

#### 3.3. Evaluation of Debye temperature

The characteristic temperature of vibration,  $\Theta$ , is related to the temperature factor of each component atom,  $B_U$  and  $B_O$ , as follows [16]

$$\frac{1}{3} (m_U B_U + 2m_O B_O) = \frac{6h^2 T}{K\Theta^2} \left( \phi(x) + \frac{x}{4} \right) \quad (4)$$

where the symbols,  $m_U$ ,  $m_O$  and  $\phi(x)$ , in Eq. (4) are the masses of uranium and oxygen atoms and the Debye function with  $x = \Theta/T$ , respectively. Although  $\Theta$  in Eq. (4) is the characteristic temperature defined by James, the value is, however, actually very close to that of the Debye temperature [16]. Therefore we treat  $\Theta$  as the Debye temperature in the following discussion. The numerical values of  $\phi(x)$  have been given in ref. [19]. It should be noted that the Debye–Waller theory must be applied to the experimental data of low temperatures. This is because the volume change of the crystal cannot be neglected at high temperature. We must, thus, take into account the effect of the thermal expansion on the calculation of the Debye temperature. The modification of the theory has been discussed by Paskin [17]. He showed that the absolute temperature in the above equation must be replaced by the reduced temperature described as

$$T' = T \left( \frac{V_T}{V_{T_0}} \right)^{2\gamma} \quad (5)$$

where  $V_T$  and  $V_{T_0}$  are the volumes of the crystal at  $T$  and the reference temperature, respectively. For  $\text{UO}_2$ , the value of the parameter  $\gamma$  in Eq. (5) is reported to be 1.7 by Clausen et al. [18].

## 4. Results and discussions

### 4.1. Temperature dependence of the temperature factor

Typical examples of the plots of  $\ln(|F_{\text{corr}}|^2/|\sum f_a|^2)$  versus  $\sin^2\theta/\lambda^2$  for several temperatures are shown in Fig. 1. Each line in the figure was drawn by a least squares fitting of the experimental data points. The sum of the atomic scattering factor,  $\sum f_a$ , was calculated as a function of the Bragg angle using the parameters listed in ref. [19]. The reflections from  $\text{CaF}_2$ -type oxide are divided into two groups. One is the group of  $\text{M} + \text{O}_2$  reflections with  $h+k+l=4n$  for which reflections from the metal and oxygen atoms are in-phase, the other is that of  $\text{M}$  reflections with  $h+k+l=4n\pm 1$  for which those from only the metal atoms. As can be seen in the figure, the data points of these two groups lie on a straight line at a fixed temperature. The figure, thus, suggests that reflection by oxygen atoms in the lattice scarcely affects the peak intensity because of its small atomic scattering factor compared with that of uranium atom.

The variation of the overall temperature factor of  $\text{UO}_2$ ,

$B$ , as a function of temperature is shown in Fig. 2. The figure shows that the value of  $B$  increases almost linearly with increasing temperature in relatively low temperature region below 1300 K. However,  $B$  has the maximum value in the vicinity of 1400 to 1500 K, and shows a rather rapid decrease with elevating temperature. The values of  $B_U$  refined by RIETAN code are plotted in Fig. 3 along with reported values [6,12,13]. Hutchings et al. examined the temperature factors  $B_U$  and  $B_O$  obtained by high temperature neutron scattering study of their own comparing with those by Albinati et al. [12] and Willis [13] over a wide temperature range from room temperature up to 2930 K [6]. They described that the value of  $B$  tended to increase with the rise of the temperature continuously [6].

Temperature dependence of  $B_U$  in Fig. 3 has almost the same inclination with that of  $B$  given in Fig. 2. In low temperature region below 1400 K, the present data well agree with the previous data [6,12,13]. Whereas, at a high temperature region between 1400 K and 1600 K in which no data points are reported, our data shows an anomalous tendency deviated from the previous data in the figure. On the other hand, the  $B_U$  at room temperature of which measurement was carried out followed by that at 1533 K was in good agreement with reported value [6]. Hence, the anomaly at high temperature shown in Figs. 2 and 3 can not be attributed to the grain growth of the sample by the heat treatment. In addition, as can be seen in Fig. 4, temperature dependence of the lattice parameter of  $\text{UO}_2$

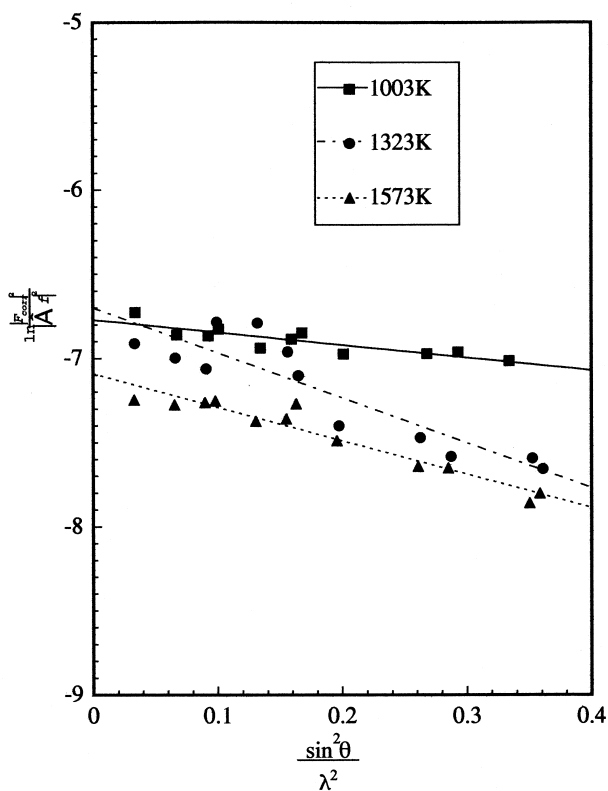


Fig. 1. Typical results of the diffraction intensity analysis of  $\text{UO}_2$ .

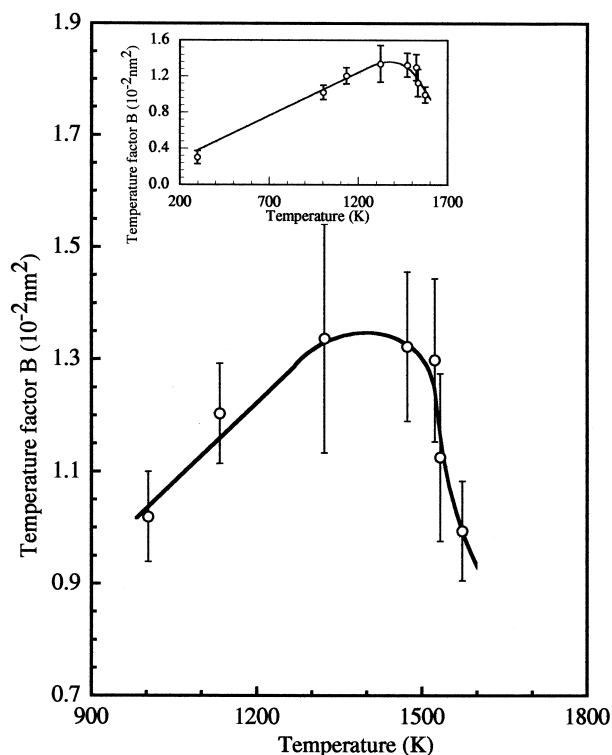


Fig. 2. Anomalous variation of overall temperature factor with increasing temperature.

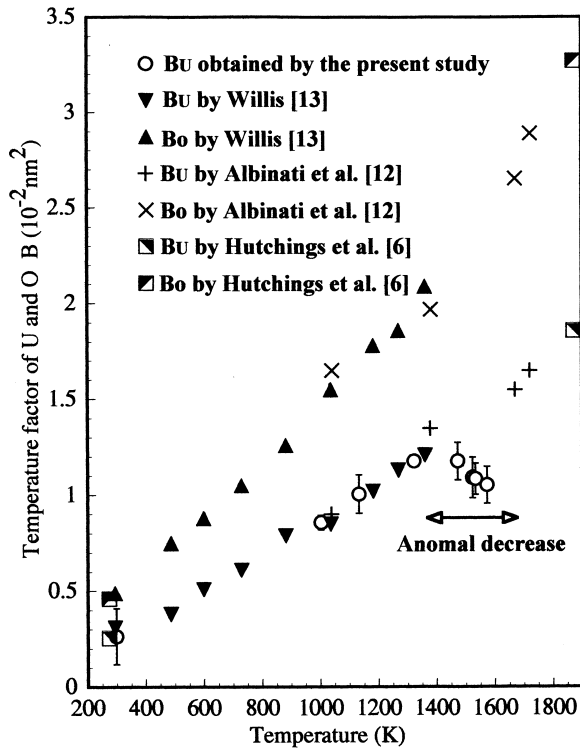


Fig. 3. Anomalous variation of the temperature factor of U atom with increasing temperature.

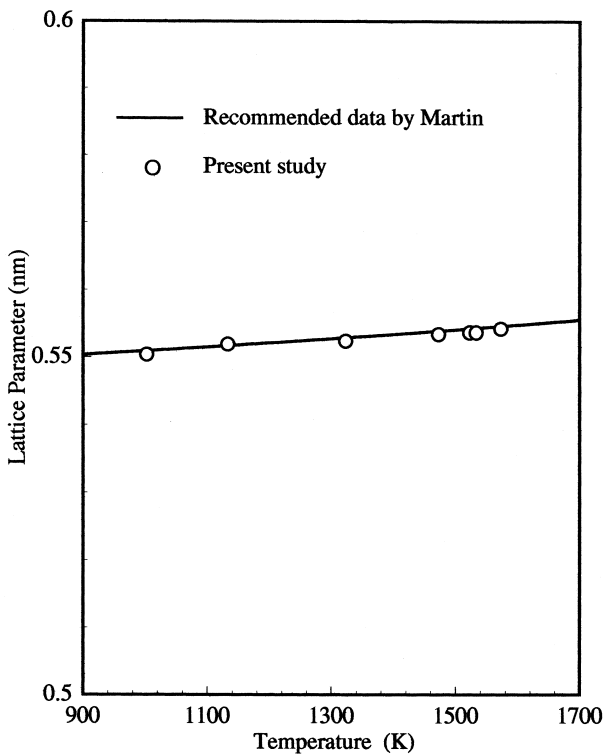


Fig. 4. Comparison of the present lattice parameter with the recommended data.

calculated from the present XRD data was well consistent with the recommended one by Martin [20]. Accordingly, the anomaly does not arise from the deviation of the optical arrangement of the diffractometer. Although the value of  $B_O$  might change with the decrease in  $B_U$ , the variation does not affect on the analysis because of the low scattering factor of O atom. The difference between our data and previous data suggests that there might be some change in electronic state of U atom. The cause of this decrease is still in question. However, there might be one reason for this anomaly. As described in Section 2, these measurements were carried out in reducing atmosphere, He/4% $H_2$  gas mixture. Therefore, the composition of the sample deviate from O/U=2.00 to O/U<2.00. If the sample was reduced to have a hypostoichiometric composition, the result of the XRD which should be affected by electronic state might differs from that of neutron diffraction.

High temperature behavior of  $UO_2$  has been intensively studied for several decades. Several workers [7–11] have revealed a pronounced increase in  $C_p$  at high temperature above around 1400 K, which is considered to be results from the formation of the anion defect or e–h pairs. Although the composition change of the sample is still in question, it is interesting that the temperature at which the anomaly in  $C_p$  occurs coincides with that at which the irregularity in the temperature factor was observed.

#### 4.2. Debye temperature

The Debye temperature,  $\Theta$ , derived from  $B_O$  and  $B_U$  is given in Fig. 5 as a function of temperature. In the temperature range from 1000 to 1400 K,  $\Theta$  obtained in the present study was almost constant, 383 K. Willis [13] has achieved the neutron diffraction study on  $UO_2$  in the temperature range of 293 to 1373 K. According to him, the Debye temperature for  $UO_2$  is independent of temperature above 673 K and equal to 377 K. The value of  $\Theta$  obtained in the present study is in good agreement with his value below 1400 K, which implies that our measurement gave basically collect values. The increase of  $\Theta$  in the temperature range between 1400 and 1573 K is non-linear and a cubical fit to our data gives the following equation:

$$\Theta = 1.89 \times 10^{-6} T^3 - 6.67 \times 10^{-3} T^2 + 7.79 T - 2.64 \times 10^3 \quad (8)$$

#### 5. Concluding remarks

High temperature behavior of  $UO_2$  was studied up to 1573 K using XRD with high temperature attachment. The values of  $B$ , and  $B_U$  increased with increasing temperature. However, an anomalous decrease was detected above ca. 1400 K, at which the excess heat capacity is observed. The corresponding Debye temperature,  $\Theta$ , also showed an

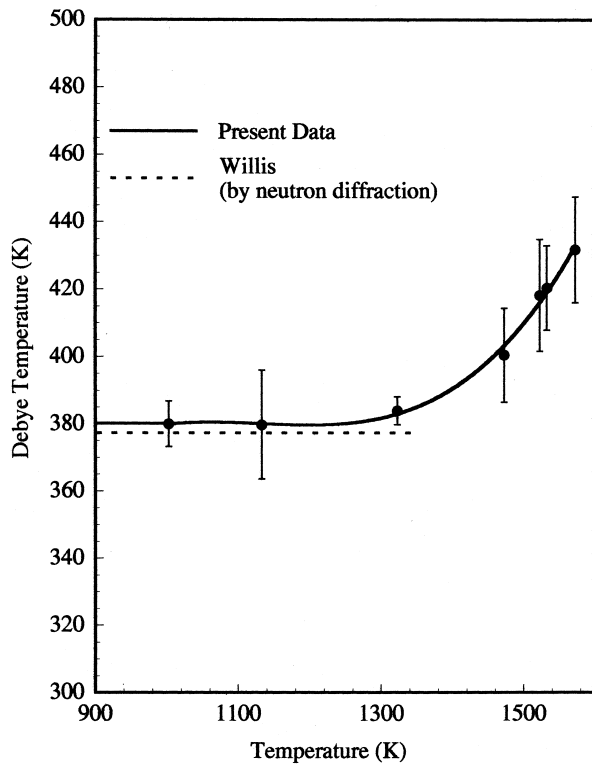


Fig. 5. Temperature dependence of Debye temperature calculated by the temperature factors,  $B_U$  and  $B_O$ .

anomalous variation with elevating temperature. Up to ca. 1400 K, however, the value of  $\Theta$  was almost constant, 383 K, which was in harmony with previous data. Above that temperature, anomalous increase in  $\Theta$  was observed up to at least 1573 K of the present measurement.

### Acknowledgements

The authors are most grateful to Dr. S. Yamanaka, Dr. T. Ogawa, Mr. Y. Ishii and Mr. S. Kashimura for their helpful

discussions and technical support. They are indebted to Dr. M. Hoshi and Dr. T. Muromura for their continuing interest and encouragement in this work.

### References

- [1] M.G. Chasanov, L. Leibowitz, S.D. Gablenick, *J. Nucl. Mater.* 49 (1973) 129.
- [2] P. Browing, *J. Nucl. Mater.* 98 (1981) 345.
- [3] G.J. Hyland, R.W. Ohse, *J. Nucl. Mater.* 140 (1986) 149.
- [4] H. J. Matzke, in: H. Blank, R. Lindner (Eds.), *Plutonium and Other Actinides*, North Holland, Amsterdam, 1976, p. 801.
- [5] M.A. Bredig, *Colloques Int. CNRS No. 205* (1972) 183.
- [6] M.T. Hutchings, K. Clausen, W. Hayes, J.E. Macdonald, R. Osborn, P. Shnabel, *High Temp. Sci.* 20 (1985) 97.
- [7] D.A. MacInnes, *J. Nucl. Mater.* 78 (1978) 225.
- [8] G.J. Hyland, J. Ralph, *High Temp. High Press.* 15 (1983) 179.
- [9] J.H. Harding, P. Masri, A.M. Stoneham, *J. Nucl. Mater.* 92 (1980) 73.
- [10] J.K. Fink, M.G. Chasanov, L. Leibowitz, *J. Nucl. Mater.* 102 (1981) 17.
- [11] J.K. Fink, *Int. J. Thermodynamics.* 3 (1982) 165.
- [12] A. Albinati, M.J. Cooper, K.D. Rouse, M.W. Thomas, B.T.M. Willis, *Acta. Cryst.* A36 (1980) 265.
- [13] B.T.M. Willis, *Proc. Roy. Soc. (London)* A274 (1963) 134.
- [14] M. J. Buerger, *Crystal Structure Analysis*, Wiley, New York, 1960, p. 231.
- [15] F. Izumi, in: R. A. Young (Ed.), *The Reitveld Method*, Chap. B, Oxford Univ. Press, Oxford, 1993.
- [16] R. W. James, *The Optical Principles of the Diffraction of X-ray*, Bell, London, 1967, p. 216.
- [17] A. Paskin, *Acta. Cryst.* 10 (1957) 667.
- [18] K. Clausen, W. Hayes, J.E. Macdonald, R. Osborn, *Rev. Phys. Appl.* 19 (1984) 719.
- [19] *International Tables for X-ray Crystallography*, Vol. IV, Kynoch Press, Birmingham, 1974, p. 99.
- [20] D.G. Martin, *J. Nucl. Mater.* 152 (1988) 94.